Journal of Membrane Science and Research 4 (2018) 20-27

Journal of Membrane Science & Research

journal homepage: www.msrjournal.com

Research Paper

High Performance Nanocomposite Cation Exchange Membrane: Effects of Functionalized Silica-Coated Magnetic Nanoparticles

Mahdi Garmsiri, Hamid Reza Mortaheb *, Mahdieh Moghadasi

Chemistry and Chemical Engineering Research Center of Iran, Tehran, P.O.Box: 14335-186

Article info

Received 2016-11-22
Revised 2017-03-11
Accepted 2017-03-11
Available online 2017-03-11

Keywords

Cation exchange membrane
Sulfonated polyethersulfone
Magnetic nanoparticles
Functionalized silica
Transport properties

Highlights

- Sulfonated PES membranes were prepared by incorporating functionalized silica-coated magnetite nanoparticles (FSMNPs).
- The prepared nanocomposite membranes were characterized and their properties were evaluated.
- Applying FSMNPs enhanced water contents, conductivities, and permselectivities of membranes.
- The nanocomposites having FSMNPs showed superior transport properties and conductivities compared to those having functionalized silica nanoparticles.

Graphical abstract

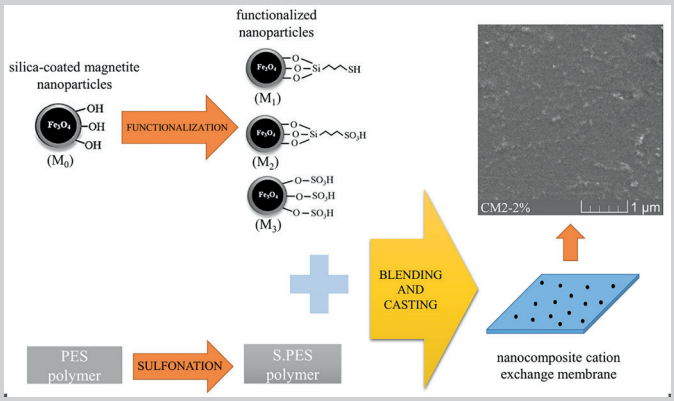

Abstract

Nanocomposite cation exchange membranes (CEMs) were prepared by adding various amounts of functionalized silica-coated magnetite nanoparticles to the sulfonated polyethersulfone (sPES) polymeric matrix. First, the particles were synthesized by the co-precipitation method (M_0). Different surface modifications were then carried out on them by grafting three functional groups of mercaptopropyl, propylsulfonic acid, and sulfonic acid to yield functionalized particles of M_1, (M_2, ion exchange capacity (IEC)= 3.09 meq.g^{-1}), and (M_3, IEC= 2.88 meq.g^{-1}), respectively. The SEM images of nanocomposite membranes verified a uniform dispersion of the nanoparticles in the membrane matrix. The nanoparticles provided more ion exchange groups and regulated water content of the membrane, and consequently enhanced its transport properties, IEC, and conductivity. The maximum values of IEC and conductivity of nanocomposite membranes were 1.8 meq.g^{-1} and 0.274 S.cm^{-1} corresponded to the membranes having 3 and 2 wt% of M_2 nanoparticles, respectively. The maximum ion conductivity of nanocomposite membrane was about two times higher than that of sPES membrane. The nanocomposite membranes containing functionalized silica-coated magnetic nanoparticles showed superior IEC, water uptake, membrane conductivity, and transport number compared to those values for the membranes containing corresponded functionalized silica nanoparticles.

1. Introduction

Cation exchange membranes (CEMs) have been used extensively in many separation processes including electrodialysis [1, 2], diffusion dialysis [3], neutralization dialysis, chloralkali process, acidic gas separation, dehumidification of gases [4, 5], fuel cells [6], batteries [7], etc. One important factor for increasing the efficiencies of the mentioned processes is improvement in transport properties of CEMs such as ionic conductivity and permselectivity. Selecting chemically and mechanically durable ion exchange membranes for applying in their harsh environments is necessary [8]. Polyethersulfone (PES) is an inexpensive polymer, which has unique characteristics such as high chemical, thermal, and mechanical stabilities [9, 10]. PES can be treated easily by using an appropriate solvent and chlorosulfonic acid to introduce sulfonic acid groups into its aromatic

* Corresponding author at: Phone: +98 21 44787751; fax: +98 21 44787781
E-mail address: mortaheb@ccerci.ac.ir (H.R. Mortaheb)

DOI: 10.22079/jmsr.2017.53303.1116

skeleton [11, 12]. The sulfonation degree of the resulted sulfonated polyethersulfone (sPES) can be adjusted by setting different reaction conditions. However, the mechanical stability of the membrane is lost in high degrees of sulfonation due to swelling and dissolving of the polymer in water [13, 14].

The physical and ion exchange properties of CEMs can be improved by using inorganic fillers such as SiO_2 [15], Al_2O_3 [16], TiO_2 [17], and carbon nanotubes [18]. Furthermore, magnetic nanoparticles (MNPs) such as Fe_3O_4 and γ-Fe_2O_3 as the inorganic fillers can be used also to surmount the limitation in membrane usage due to high swelling, degradation of sulfonic groups in harsh temperature conditions, and insufficient thermal stability. These characteristics introduce them as the good candidates to improve the properties of nanocomposite membranes [19, 20]. Different structures of iron oxide including magnetite (Fe_3O_4), maghemite (γ-Fe_2O_3), and hematite (α-Fe_2O_3) induce various magnetic properties depending on temperature, crystallinity, particle size, and cation substitution [21]. Although magnetite and maghemite both display good magnetic properties in room temperature [22, 23], Fe_3O_4 nanoparticles are preferred as they can be prepared by less synthesis steps [24].

Meanwhile, Fe_3O_4 is chemically active and can be easily oxidized by air causing it to lose its dispersibility, which can deteriorate its contribution in enhancing the membrane conductivity. A coating material such as silica not only chemically stabilizes the metallic nanoparticles but also prevents them to be agglomerated. Furthermore, it allows introducing desire functional groups to the surface of the nanoparticle [25, 26]. Therefore, The silica-coated MNP as a combination of two inorganic material (Fe_3O_4 and SiO_2) influences CEMs properties in different ways by adding surface functional groups on the nanoparticle surfaces [27].

On the other hand, some literatures report enhancement of membrane conductivity by using electric and magnetic fields during the membrane formation step [28-30]. The interactions of surface groups on the nanoparticle and the side chain sulfonic acid groups of the polymeric matrix in a magnetic field can create pathways for transportation of ions and facilitate the ion transportation along the membrane [31]. In other words, applying magnetic field helps to a better dispersion and alignment of silica-coated MNPs along the direction of magnetic field and to establish shorter and ordered paths for transportation of ions and decrease the blocking effect in the membrane matrix [32, 33].

Functionalizing silica-coated MNPs contributes new interfacial interactions with polymeric molecules and helps creating new molecular arrangement so that the properties of composite membranes can be modified [34, 35]. Moreover, by optimizing water content and the *IEC* of the membrane, higher conductivity and permselectivity are gained [36-38].

In the present research, the transport properties of nanocomposite membranes are enhanced by exploiting the benefits of proper dispersion and arrangement of the nanoparticles in the membrane matrix. The magnetic (Fe_3O_4) nanoparticles are synthesized and then coated by silica. The coated MNPs are functionalized by mercaptopropyl, sulfonic acid, and propyl sulfonic acid groups. The functionalized coated MNPs with high *IEC* are then added to the membrane matrix. Finally, the effects of nanoparticles with various functional groups on the properties of nanocomposite such as membrane morphology, thermal stabilities, *IEC*, water uptake, porosity, contact angle, transport number, membrane permselectivity, and concentration of fixed charges on the membrane surface membranes are investigated.

2. Experimental

2.1. Materials

All reagents used in the present research were of analytical grade. Polyethersulfone (Ultrason E6020, Mw=58,000) was provided by BASF, Germany. $FeCl_2.4H_2O$, $FeCl_3.6H_2O$, H_2SO_4, HCl, NaOH, hydrogen peroxide solution (30 wt%), ammonium hydroxide solution (32 wt%), tetraethyl orthosilicate (TEOS), chlorosulfonic acid, phenolphthalein, methanol, ethanol, N,N-Dimethylacetamide (DMAc), and dichloromethane were purchased from Merck, Germany. (3-Mercaptopropyl) trimethoxysilane (MPTMS) was purchased from Sigma-Aldrich. All chemicals were used as received and without further purifications.

2.2. Synthesis and functionalization of silica-coated magnetite nanoparticles

The MNPs were synthesized by a co-precipitation procedure as described in literature [39]. Firstly, $HCl.H_2O$ (0.85 ml, 30%) was added to 25 ml deionized water. Then, $FeCl_3.6H_2O$ (3.12 g) and $FeCl_2.4H_2O$ (2 g) were dissolved in the solution under nitrogen gas at 80 °C. The NaOH solution (250 ml, 1.5 M) was added to the solution and stirred for 1 h until the magnetite precipitates were formed (Eq. (1)). The precipitates were collected, washed by deionized water several times, and then dried in a vacuum oven at 60 °C for 2 h.

$$2Fe(III) + Fe(II) + 8OH^- \Rightarrow Fe_3O_4 + 8H_2O \quad (1)$$

In the next step, in order to coat the MNPs with a thin layer of silica, 0.4 g of the particles were dispersed completely in ethanol (150 ml) by ultrasonic stirring for 45 min [40]. $NH_3.H_2O$ (24 ml, 32 wt%) and TEOS (0.8 g) were added to the solution and sonicated for 2 h. A layer of silica was formed on the particles. The silica-coated MNPs were then washed three times by ethanol, and dried in the vacuum oven for 2 h. The mechanisms of coating reactions are as follows [40]:

$$Si(OR)_4 + 4H_2O \Rightarrow Si(OH)_4 + 4ROH \quad (2)$$

$$nSi(OH)_4 \Rightarrow n(SiO_2) + 2nH_2O \quad (3)$$

The surface grafting of silica-coated MNPs were carried out according to the procedure in literature [41-43]. The silica-coated MNPs (M_0) were dried in the vacuum oven at 150 °C to remove adsorbed surface water. In the first step, the M_0 nanoparticles (1.2 g) were added to a mixture of dry toluene (14 ml) and MPTMS (2.4 g) and were refluxed for one day at 110 °C. The resultant nanoparticles (M_1) were washed by dry toluene and acetone, and then were dried in the vacuum oven at 70 °C. In the second step, the thiol groups of the papered M_1 nanoparticles were converted into sulfonic acid groups by oxidizing in a solution of 30% H_2O_2 at 60 °C for one day. The nanoparticles were washed by a solution of 0.1 M sulfuric acid and the additional acidic agents were removed by multiple washing with a mixture of water and ethanol. Finally, the nanoparticles (M_2) were dried in room temperature.

The direct functionalization of silica coatings by sulfonic acid groups was done by adding chlorosulfonic acid (0.7 g) to a mixture of dichloromethane (7 ml) and silica nanoparticles (0.35 g). The mixture was stirred at room temperature for 30 min. The nanoparticles (M_3) were then filtered and washed by a mixture of water and ethanol and dried at room temperature. The schemes of reactions are summarized in Figure 1.

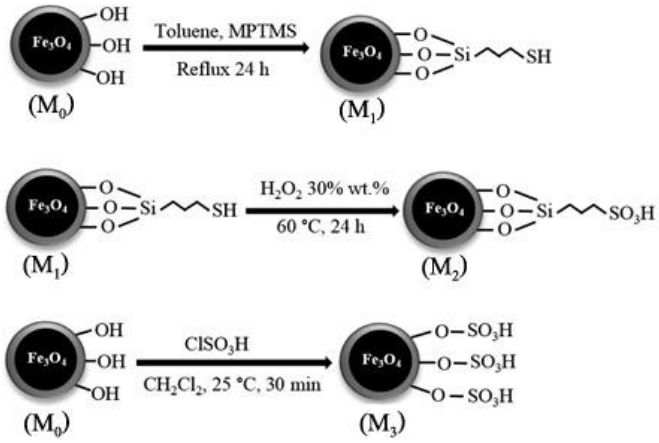

Fig. 1. Schemes of functionalization of silica-coated magnetic nanoparticles.

2.3. Membrane preparation

The sulfonation process of PES was performed according to the procedure in literature [11, 13]. The PES powder (20 g) was dissolved in sulfuric acid (108.7 ml) and then chlorosulfonic acid (113.3 g) was gently added to the solution and stirred at room temperature for 9 h. The cold water was added to the solution dropwise until sPES was participated. The polymeric precipitate was washed by deionized water several times and dried in the vacuum oven for 1 day at 70 °C.

The nanocomposite membranes were prepared by casting and solvent-evaporation processes. The weight percent ratios of sPES/MNPs were 20/(0.1, 0.5, 1, and 2), respectively. sPES was added to the solvent (DMAc) and stirred until the polymer was dissolved. The MNPs were also dispersed in the solvent by stirring and sonication for 30 min. The mixtures were mixed

together by stirring and sonication for 2 h. The casting solution was degassed by keeping in stagnant conditions for 2 h at 50 °C. The viscous polymeric solution was then cast on a glass using a doctor blade. In order to aligning silica-coated MNPs in the membrane matrix, a uniform perpendicular magnetic field (0.15 T) was applied during the casting step for few hours. The cast solution was put in the vacuum oven for 12 h at 60 °C and temperature was raised to 75 °C for 8 h. The membranes were immersed in 1 M HCl for one day and washed with deionized water several times. Each membrane was equilibrated with the working solution before the tests. The membranes were named as CX-Y% where X is type of nanoparticle include (M_0, M_1, M_2, and M_3), and Y is the silica content (wt%) in the nanocomposite membrane.

2.4. Characterization methods

2.4.1. Structural and morphological studies

The Fourier transform infrared (FTIR) spectra were obtained by Perkin-Elmer 883, USA. The sPES membranes were studied by IR absorption spectra with a resolution of 4 m^{-1} and wave number range of 4000–400 cm^{-1}.

The structural properties of magnetic nanoparticle were studied by X-ray diffraction under Cu Kα radiation (40 kV, 40 mA, range of 2Θ=4-70).

Field emission scanning electron microscopy was applied to investigate the structure of silica-coated nanoparticles and nanocomposite membranes under accelerating voltage of 20 KV. The samples were prepared by wiping out of the membrane surface, fracturing in liquid nitrogen, and gold sputtering.

2.4.2. Ion exchange capacity, water uptake, and membrane porosity

The *IEC* of the composite membrane was calculated by back titration using standard solutions of HCl and NaOH, and phenolphthalein as the indicator. The membrane was washed and then equilibrated by a 1 M HCl solution for one day. The excess H^+ was removed by washing and immersing the membrane in deionized water for one day. The membrane was dipped in a 0.01 M NaOH solution for one day and then titrated by a 0.01 M HCl solution. The membrane was washed, immersed in the deionized water, cleaned after washing, and then immersed in the deionized water to determine the wet weight of the membrane. The membrane was dried in the vacuum oven until no further weight losses was observed. The dry weight of the membrane was then measured. The *IEC* (meq.g^{-1}) and water uptake (φ_w) of the membrane were obtained using the following equations:

$$IEC = \frac{V_s \times C_{H^+}}{W_{dry}} \tag{4}$$

$$\varphi_w = \frac{w_{wet} - w_{dry}}{w_{dry}} \tag{5}$$

where V_s is the volume of the solution, C_{H^+} is the concentration of H^+, and w_{wet} and w_{dry} are the weights of wet and dry membranes, respectively.

The volume of free water within the membrane per unit volume of the dry membrane (ΔV), and the membrane porosity (τ_m) are calculated using the following equations:

$$\Delta V = \frac{(w_{wet} - w_{dry}) \cdot \rho_d}{\rho_w \cdot w_{dry}} \tag{6}$$

$$\tau_m = \frac{\Delta V}{\Delta V + 1} \tag{7}$$

where ρ_d and ρ_w are the densities of dry membrane and water, respectively.

2.4.3. Contact angle

The hydrophilicity of the membrane's surface was determined by an optical contact angle measurement device (OCA-20, Dataphysics, Germany). Five randomly selected points were used for the measurements to minimize the experimental error and the average value was reported.

2.4.4. Membrane potential

The membrane potential was measured by Ag/AgCl reference electrodes and digital multimeter in room temperature (25°C). The measurement setup contained two cylindrical glass cells where the membrane with 7.70 cm^2 effective area was placed between them. To eliminate the effect of boundary layers, the solutions were stirred intensely. The counter-ion transport number in the membrane, t_c^m, can be derived from the following equation:

$$E_m = \frac{RT}{F}(2\,t_c^m - 1)\ln\left(\frac{C_1}{C_2}\right) \tag{8}$$

where E_m is the membrane potential and C_1 and C_2 are concentrations of NaCl solutions in the two sides of the membrane (C_2/C_1=5, C_1= 0.01, 0.02, and 0.1 mol/L).

The selectivity between co-ion and counter-ion is expressed by the permselectivity term. The permselectivity (P_s) and concentration of fixed charges on the membrane surface (X_m) are calculated by the following equations, respectively:

$$P_s = \frac{t_c^m - t_c}{1 - t_c} \tag{9}$$

$$X_m = \frac{2\,C_s\,P_s}{\sqrt{1 - P_s^2}} \tag{10}$$

where t_c is the transport number of counter-ion in the solution phase and C_s is the mean electrolyte concentration.

2.4.5. Membrane conductivity

The membrane conductivity was evaluated by a potentiostat/galvanostat frequency response analyzer (Auto Lab, Model PGSTAT 30) according to in-plane configuration [44]. Before measurement, the membrane was equilibrated in a 0.5 M NaCl solution. The conductivity was obtained in the same solution where the frequency and the excitation signal were set to 100 Hz-100 kHz and 10 mV, respectively. The membrane conductivity is determined by the following equation:

$$\sigma = \frac{L}{A.R} \tag{11}$$

where A is the membrane cross-sectional area, L is the distance between two electrodes, and R is the membrane resistance.

2.4.6. Thermogravimetric analysis

The thermal stability of the membranes and nanoparticles were studied using thermogravimetric analysis (TGA) (TG 209 F1 Iris, NETZCH, Germany) under nitrogen gas flow (25 mL.min^{-1}) in the heating range of 25-800 °C.

3. Results and discussion

3.1. Polymer characterization

The FTIR spectra of sPES are shown in Figure 2. Two absorption peaks observed at 1650 cm^{-1} and 1431 cm^{-1} are related to vibration of the aromatic ring skeleton. The absorption peaks of hydroxyl group, aromatic sulfone group, and aryl oxide are appeared at ~3433 cm^{-1}, ~1156 cm^{-1}, and ~1243 cm^{-1}, respectively. The absorption peak related to asymmetrical stretching vibration of sulfonic acid group overlaps with the aromatic sulfone group.

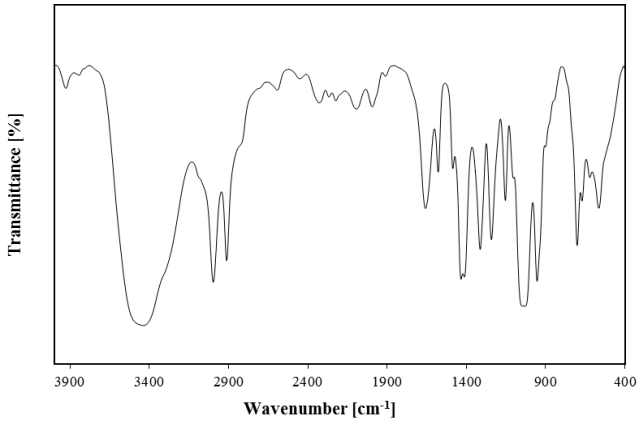

Fig. 2. FTIR spectra of synthesized sPES.

3.2. Characterization of nanoparticles

The morphologies of functionalized silica-coated MNPs are shown in Figure 3. The average particle size is in the range of 120-180 nm. The nanoparticles are uniform in shape and no significant changes are observed after functionalization.

Among the coatings used in preparation of MNPs, M_2 and M_3 can contribute in ion exchanging due to the presence of sulfonic acid groups in their structures. The *IEC*s of M_2 and M_3 nanoparticles measured by the titration method are 3.09 and 2.88 meq.g^{-1}, respectively. Although, M_3 has more sulfonic acid groups in its structure compared to M_2, existing propyl chain in the structure of M_2 provides more activity to the ion exchange groups, i.e., sulfonic acid groups of M_2 and thus a relatively higher *IEC*.

X-ray diffraction (XRD) spectroscopy of nanoparticles (see Figure 4) shows diffraction peaks at 30.2˚, 35.6˚, 43.2˚, 57.1˚, and 62.8˚, which are corresponded to magnetite cubic spinal structure of Fe_3O_4 nanoparticles confirming the high purity of the phase and that the crystallinity of magnetic core has been retained after the coating process.

TG analyses of the silica-coated MNPs are shown in Figure 5. The first weight change around 100˚C is corresponded to the loss of physically-adsorbed water in nanoparticles. A higher loss around 100˚C is observed for M_2 and M_3 nanoparticles due to their higher water contents because of existing more acidic groups in their structures. Degradation of alkoxy groups causes a further loss around 300˚C for M_1, M_2 and M_3 nanoparticles. Weight losses around 550°C is related to the oxidation of nanoparticles' coatings.

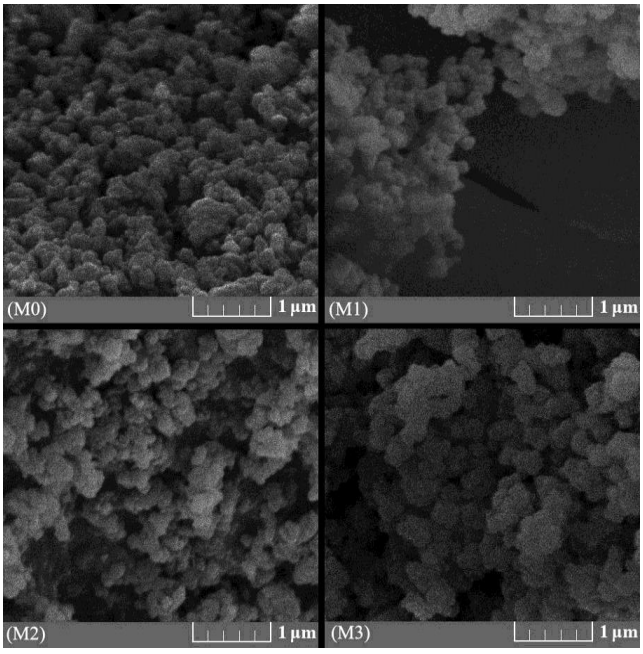

Fig. 3. SEM images of functionalized silica-coated MNPs.

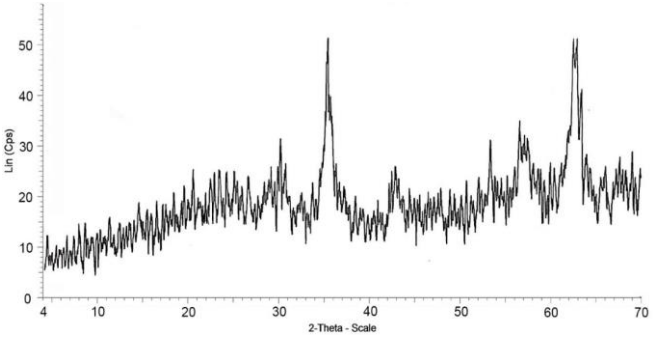

Fig. 4. XRD spectra of functionalized silica-coated MNPs.

3.3. Characterization of nanocomposite membranes

3.3.1. Membrane morphology

The surface and cross sectional SEM images of nanocomposite membranes having 0.5 and 2 wt % nanoparticles are shown in Figure 6. The nanoparticles can change the morphology of membrane's surface and provide higher ion exchange sites and water contents. No pores or phase separations are observed in the cross section images of the membranes. Since the acidic groups of nanoparticles may form bonds with hydrophilic sites of the polymeric matrix, also because of applying a uniform magnetic field across the membrane during the membrane preparation step, a uniform dispersion of nanoparticles with no aggregation is observed on the surfaces of membranes.

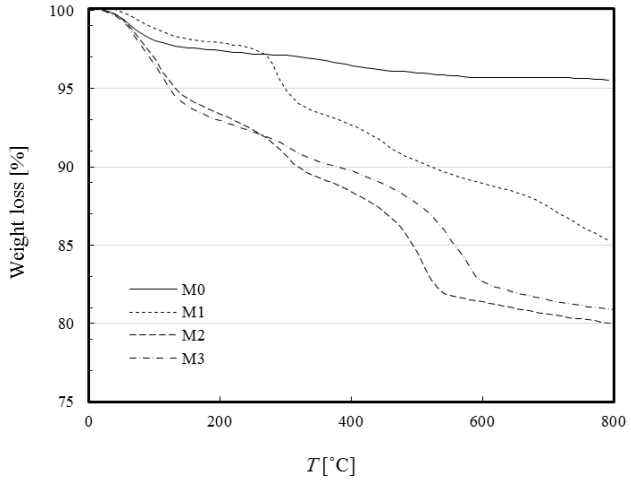

Fig. 5. TG analysis of functionalized silica-coated MNPs.

3.3.2. TGA of nanocomposite membranes

The thermal stabilities of nanocomposite membranes were investigated by TGA for the membranes having 2 wt% nanoparticle (see Figure 7). The weight loss around 100˚C is corresponded to the physically-adsorbed water. For sPES, CM_0-2%, and CM_1-2%, the weight losses around 350˚C are related to thermal decomposition of sulfonic acid groups and functional groups of M_1. For CM_2-2% and CM_3-2%, the membranes weight losses around 250˚C are assigned to the decomposition of sulfonic acid groups in the membranes and nanoparticles. Degradation of polymeric matrix is occurred around 470-520˚C. All membranes showed adequate thermal stabilities. However, the thermal stabilities of CM_2-2% and CM_3-2% membranes are decreased slightly due to presence of more acidic groups.

3.3.3. IEC, water uptake, and contact angle

IEC, water uptake, contact angle, and porosity of the prepared nanocomposite membranes are reported in Table 1. Introducing functionalized silica nanoparticles affects the content of sulfonic acid groups and changes the *IEC*s of nanocomposite membranes. Higher contents of nanofillers establish more microscopic free volume, increase the hydrophilic groups, and enhance the tendency of nanoparticles to adsorb more water in the membranes. As could be observed in Table 1, adding nanoparticles to the membrane matrix increases the water uptake and porosity of the membranes. Due to lack of acidic groups in M_0 and M_1 nanoparticles, *IEC*s with lower values are gained for CM_0 and CM_1 membranes. Acidic nanoparticles raise the *IEC* up to 1.803 and 1.788 for CM_2 and CM_3 membranes, respectively. The morphologies of membranes' surfaces and acidic group concentrations are not changed in a wide range and thus it is expected that the contact angles of the membranes do not change significantly.

3.3.4. Membrane conductivity

The silica-coated MNPs can enhance the conductivity and exchange properties of the membrane. The membrane conductivity, which depends on many factors such as membrane structure and the type of mobility ions, is increased by increasing *IEC* and water uptake of the membrane. Figure 8 shows the conductivities of the nanocomposite membranes. By adding M_0 and M_1 nanoparticles, the conductivities of the membranes are decreased. This is due to lack of ion exchange groups in those nanoparticles and the blocking effect in higher contents. In low contents of nanoparticles, the decrement in conductivity is retarded when M_1 (having thiol group in its structure) is added comparing to that when M_0 is added. However, the reduction in the conductivity of CM_1 is accelerated in higher contents.

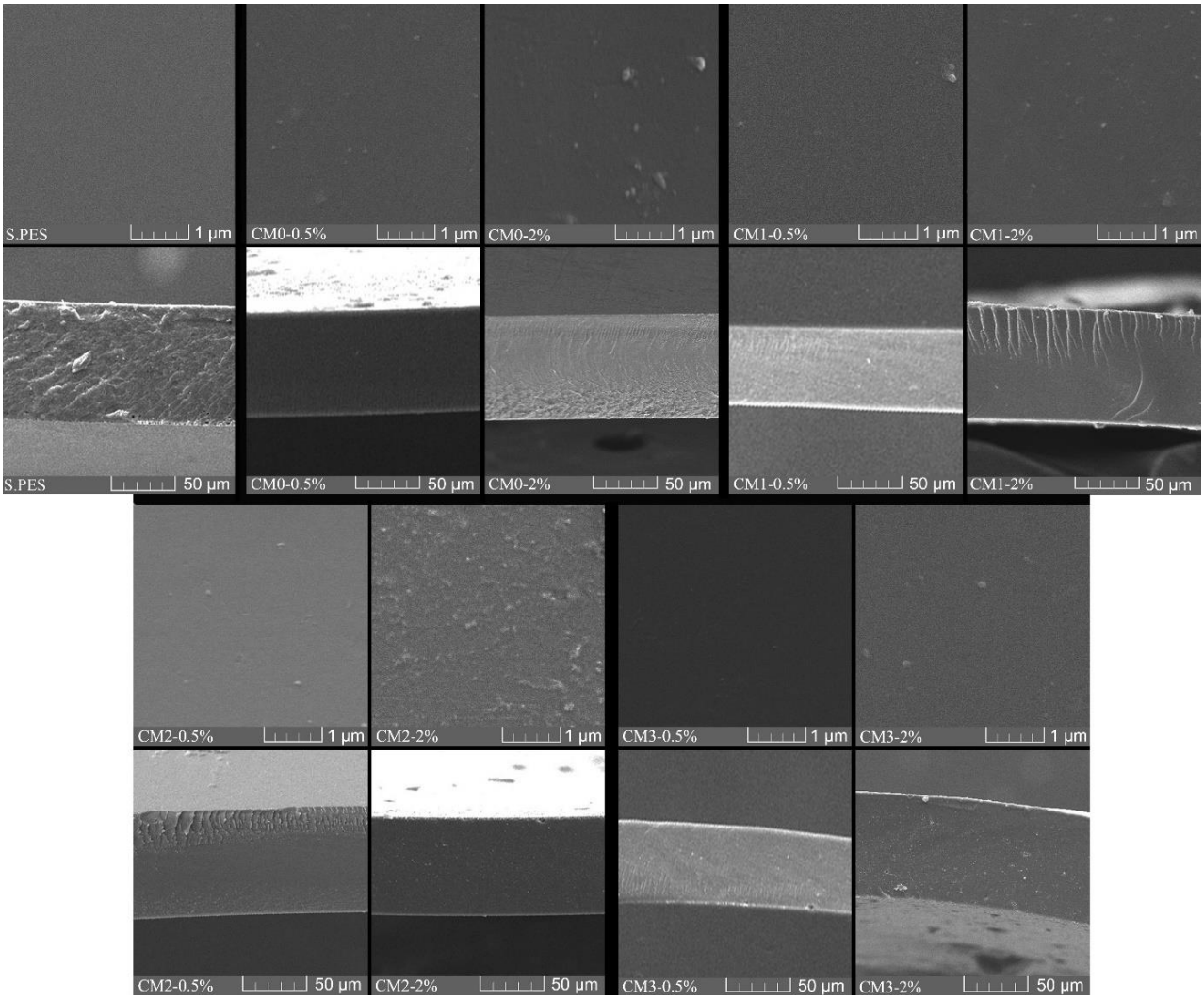

Fig. 6. Surface and cross sectional SEM images of nanocomposite membranes.

Table 1
IEC, water uptake, porosity, and contact angle of nanocomposite CEMs.

Sample	*IEC* [meq.g^{-1}]	Water uptake [-]	Porosity [-]	contact angle [°]
sPES	1.689	0.238	0.194	83.43
CM_0-0.1%	1.702	0.292	0.194	83.84
CM_0-0.5%	1.626	0.256	0.193	84.89
CM_0-1%	1.625	0.325	0.231	85.19
CM_0-2%	1.515	0.326	0.244	85.50
CM_1-0.1%	1.685	0.402	0.236	85.93
CM_1-0.5%	1.667	0.489	0.279	86.10
CM_1-1%	1.630	0.465	0.284	86.29
CM_1-2%	1.597	0.506	0.275	87.36
CM_2-0.1%	1.712	0.413	0.248	86.15
CM_2-0.5%	1.708	0.403	0.254	87.51
CM_2-1%	1.720	0.462	0.278	87.60
CM_2-2%	1.803	0.492	0.285	87.60
CM_3-0.1%	1.663	0.288	0.177	84.30
CM_3-0.5%	1.661	0.419	0.263	85.79
CM_3-1%	1.755	0.472	0.269	86.44
CM_3-2%	1.788	0.461	0.274	87.23

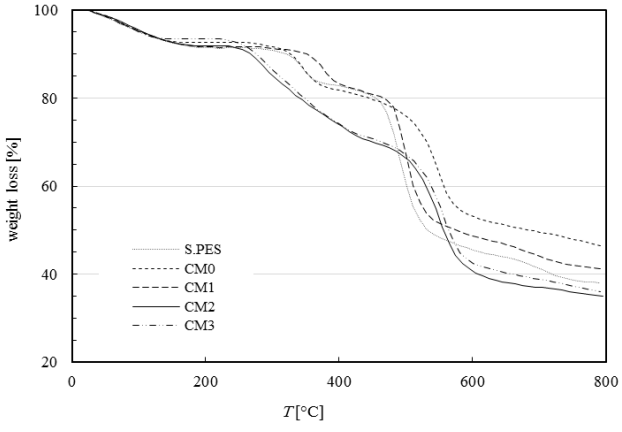

Fig. 7. TG analysis of sPES and nanocomposite CEMs with 3 wt% nanoparticle.

On the other hand, adding M_2 and M_3 to the membrane structure increases the membrane conductivity up to 0.274 and 0.251 [S.cm^{-1}], respectively. Such an observation may be due to increase in ion exchange groups and adjusting the water contents by adding those fillers. In comparison between CM_2 and CM_3 nanoparticles, CM_2 shows a higher conductivity due to higher cation exchange groups and water content in the membrane matrix.

3.3.5. Electric potential

Difference in electrolyte concentrations between the two sides of the membrane creates an electrical potential for ion transportation across the membrane. The transport number is defined as the fraction of the current passes through the membrane by counter-ion. The transport number depends on the kinds and mobilities of co-ions and counter-ions, membrane properties, and the electrolyte concentration. Selective passage of ions is expressed by the permselectivity term, which is affected by interactions between co-ions/counter-ions and the membrane matrix [45, 46]. The transport number, permselectivity, and fixed charges on the membrane surface are shown in Table 2. The transport number is decreased in higher concentrations of electrolyte solution due to decreased Donnan exclusion. By adding nanoparticles to the membranes, all parameter including transport number, membrane permselectivity, and the concentration of fixed charges on the membrane surface are increased. Transport mechanism can be very complicated in presence of functionalized nanoparticles and may depend on water content, *IEC*, interaction between the fillers and polymeric matrix, and the membrane's nature [44, 46]. CM_1 and CM_2 membranes show higher transport numbers and permselectivities.

Table 2
Transport number, membrane permselectivity, and concentration of fixed charges on the membrane surface of nanocomposite membranes.

C_1 (*mol* dm^{-3})	0.01			0.02			0.1		
	t_c^m	P_s	X_m	t_c^m	P_s	X_m	t_c^m	P_s	X_m
sPES	0.906	0.845	0.095	0.893	0.823	0.174	0.888	0.815	0.844
CM_0-0.1%	0.905	0.843	0.094	0.9	0.835	0.182	0.899	0.833	0.904
CM_0-0.5%	0.913	0.855	0.099	0.908	0.847	0.191	0.9	0.835	0.911
CM_0-1%	0.948	0.913	0.134	0.929	0.883	0.226	0.917	0.863	1.026
CM_0-2%	0.955	0.925	0.146	0.942	0.903	0.253	0.934	0.891	1.179
CM_1-0.1%	0.929	0.883	0.113	0.925	0.875	0.217	0.913	0.855	0.99
CM_1-0.5%	0.942	0.903	0.126	0.929	0.883	0.226	0.917	0.863	1.026
CM_1-1%	0.948	0.913	0.134	0.934	0.891	0.236	0.923	0.873	1.075
CM_1-2%	0.957	0.929	0.151	0.95	0.917	0.276	0.944	0.907	1.294
CM_2-0.1%	0.899	0.833	0.09	0.893	0.823	0.174	0.881	0.803	0.808
CM_2-0.5%	0.929	0.883	0.113	0.923	0.873	0.215	0.917	0.863	1.026
CM_2-1%	0.954	0.923	0.144	0.949	0.915	0.273	0.942	0.903	1.263
CM_2-2%	0.973	0.955	0.194	0.968	0.947	0.355	0.962	0.937	1.613
CM_3-0.1%	0.906	0.845	0.095	0.893	0.823	0.174	0.888	0.815	0.844
CM_3-0.5%	0.918	0.864	0.103	0.905	0.843	0.188	0.899	0.893	1.193
CM_3-1%	0.936	0.893	0.119	0.913	0.855	0.198	0.9	0.896	1.207
CM_3-2%	0.942	0.903	0.126	0.929	0.883	0.226	0.917	0.926	1.473

Table 3
Characterization of membranes having silica-coated MNPs (CMs) and silica NPs (CSMs).

Sample	*IEC* [meq.g^{-1}]	Water uptake [-]	Porosity [-]	σ [S.cm^{-1}]	t_c^m [-] at C_1 = 0.1 mol/L
CSM_2-1%	1.702	0.355	0.268	0.232	0.955
CSM_3-1%	1.679	0.330	0.222	0.181	0.882
CSM_2-2%	1.696	0.378	0.267	0.110	0.923
CSM_3-2%	1.699	0.323	0.228	0.244	0.881
CM_2-1%	1.720	0.462	0.278	0.245	0.942
CM_3-1%	1.755	0.472	0.269	0.228	0.900
CM_2-2%	1.803	0.492	0.285	0.274	0.962
CM_3-2%	1.788	0.461	0.274	0.251	0.917

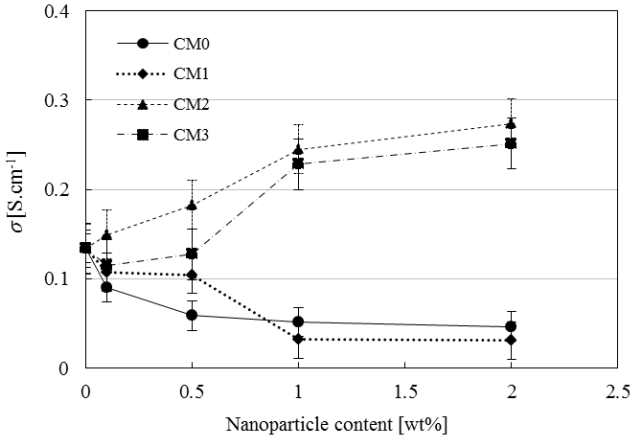

Fig. 8. Conductivities of nanocomposite membranes.

3.3.6. Comparison between properties of membranes containing silica-coated magnetic nanoparticles and silica nanoparticles

The effect of magnetic field was investigated by comparison the performances of membranes having silica-coated magnetic nanoparticles and those having silica nanoparticles. The characterizations of the membranes for 1 and 2 wt% nanoparticle contents are summarized in Table 3. The membranes having silica nanoparticles are represented as CSX-Y% where X is type of functionalized silica and Y is its weight percent. It is noticeable that the size of applied silica nanoparticle was 80 nm and the *IEC*s of SM2 and SM3 nanoparticles were 2.71 and 2.84 meq.g^{-1}, respectively. The results in Table 3 show that although the porosities of the two membrane types do not change significantly, the water uptakes are higher for the membranes having silica-coated MNPs, which can be due to the nature of nanoparticles and membrane formation conditions. The results also show that both conductivity and transport number of the membranes having coated MNPs are higher than those having silica NPs. Three factors may be considered for such an observation: 1) ion exchange capacity, 2) water uptake, and 3) arrangement of nanoparticles [27]. Because of the high values of ion exchange capacities in the membrane matrices, higher water uptake and enhanced arrangement of the coated magnetic nanoparticles along the magnetic field may be considered as the controlling parameters, which can reduce the resistance against ion transport in the membrane [35, 36].

3.3.7. Comparison between performances of present membranes and previous ones

Table 4 summarizes a comparison between maximum values of *IEC*, water uptake, membrane conductivity, and transport number obtained in the present research and those of previous studies. Although the presence of different ionomers and fillers leads to different properties, the values in the table indicate a superior performance for the prepared membranes in the present research.

4. Conclusions

Magnetic nanoparticles were synthesized and coated by silica nanoparticles. This modification enabled the nanoparticles to be functionalized by different agents and prevented from their agglomeration.

The nanocomposite membranes were synthesized by adding functionalized nanoparticles to the polymeric matrix of sPES. The SEM images confirmed that the nanoparticles were uniformly dispersed in the membranes. Due to higher *IEC*s of the acidic nanoparticles, the *IEC* of the membrane could be increased from 1.689 for the unfilled sPES membrane up to 1.803 meq.g^{-1} for the nanocomposite membrane (CM_2-2%) while *IEC*s of CM_0 and CM_1 membranes were lower than that of sPES membrane. TG analyses showed that the nanocomposite membranes have appropriate thermal stabilities. Water uptakes and porosities of as high as 0.506 and 0.285 could be obtained for the nanocomposite membranes by adding different amounts of the nanoparticles, which are higher than those for the unfilled sPES membrane (0.238 and 0.194, respectively). Adding nanoparticles had positive effects on the conductivity of nanocomposite membranes due to their higher *IEC* and water uptake especially for CM_2 (0.274 S.cm^{-1} at 2%) and CM_3 (0.252 S.cm^{-1} at 2%). The transport properties including transport number and permselectivity were improved by increasing the nanoparticle content. A comparison between *IEC*, water uptake, membrane conductivity, and transport number for the nanocomposite membranes containing functionalized silica-coated magnetic nanoparticles and those containing corresponded functionalized silica shows superior properties of the prepared membranes having coated magnetic nanoparticles.

All in all, the present research reveals how much adding the silica-coated MNPs can enhance the transport properties of composite membranes by contributing the properties of both magnetic particles and inorganic coatings as well as the grafted functional groups.

Table 4
Comparison between maximum values of *IEC*, water uptake, membrane conductivity, and transport number for prepared nanocomposite membranes in present research and those of previous ones.

Ref.	Polymer/Particle	*IEC* [meq.g^{-1}] at particle content [wt%]	Water uptake [%] at particle content [wt%]	Conductivity [mS.cm^{-1}] at particle content [wt%] (solution condition)	Transport number (Na^+) [-] at particle content [wt%]
[27]	sPES/montmorillonite	1.80 at 0%	-	16.0 at 0% (fully hydrated)	-
[16]	sPES/γ-Fe_2O_3	1.59 at 0%	28.1 at 0%	14.5 at 0% (fully hydrated)	-
[17]	sPES/sulfonated mesoporous silica	1.10 at 0.2%	14.3 at 0.2%	0.24 at 1% (0.5 mol.dm^{-3} NaCl)	1.00 at 0.5%
[42]	sPES/graphene oxide	1.40 at 0%	15.2 at 10%	0.06 at 10% (water)	0.96 at 10%
Present work	S.PES/functionalized SiO_2	1.90 at 3% of M_3	39.8 at 0.5% M_2	29.3 at 2% M_3 (0.5 mol.dm^{-3} NaCl)	0.98 at 1% M_2

References

[1] N. Yamada, T. Yaguchi, H. Otsuka, M. Sudoh, Development of trickle-bed electrolyzer for on-site electrochemical production of hydrogen peroxide, J. Electrochem. Soc. 146 (1999) 2587-2591.

[2] T. Wen, G.S. Solt, Y.F. Sun, Modelling the cross flow spirally wound electrodualysis (SpED) process, Desalination, 103 (1995) 165-176.

[3] Y. Journal of Electroanalytical ChemistryKobuchi, H. Motomura, Y. Noma, F. Hanada, Application of ion exchange membranes to the recovery of acids by diffusion dialysis, J. Membr. Sci. 27 (1986) 173-179.

[4] R.K. Nagarale, G.S. Gohil, V.K. Shahi, Recent developments on ion-exchange membranes and electro-membrane processes, Adv. Colloid Interface Sci. 119 (2006) 97-130.

[5] F. Fu, Q. Wang, Removal of heavy metal ions from wastewaters: A review, J. Environ. Manage. 92 (2011) 407-418.

[6] M.A. Hickner, H. Ghassemi, Y.S. Kim, B.R. Einsla, J.E. McGrath, Alternative polymer systems for proton exchange membranes (PEMs), Chem. Rev. 104 (2004) 4587-4612.

[7] D. Chen, M.A. Hickner, E. Agar, E.C. Kumbur, Optimized anion exchange membranes for vanadium redox flow batteries, ACS Appl. Mater. Interfaces, 5 (2013) 7559-7566.

[8] T. Xu, Ion exchange membranes: State of their development and perspective, J. Membr. Sci. 263 (2005) 1-29.

[9] A.F. Ismail, W.J. Lau, Theoretical studies on structural and electrical properties of PES/SPEEK blend nanofiltration membrane, AlChE J. 55 (2009) 2081-2093.

[10] C. Klaysom, S.-H. Moon, B.P. Ladewig, G.Q.M. Lu, L. Wang, Preparation of porous ion-exchange membranes (IEMs) and their characterizations, J. Membr. Sci. 371 (2011) 37-44.

[11] R. Guan, H. Zou, D. Lu, C. Gong, Y. Liu, Polyethersulfone sulfonated by chlorosulfonic acid and its membrane characteristics, Eur. Polym. J. 41 (2005) 1554-1560.

[12] M.-S. Kang, Y.-J. Choi, I.-J. Choi, T.-H. Yoon, S.-H. Moon, Electrochemical characterization of sulfonated poly(arylene ether sulfone) (S-PES) cation-exchange membranes, J. Membr. Sci. 216 (2003) 39-53.

[13] H. Dai, R. Guan, C. Li, J. Liu, Development and characterization of sulfonated poly(ether sulfone) for proton exchange membrane materials, Solid State Ionics, 178 (2007) 339-345.

[14] K. Matsumoto, T. Nakagawa, T. Higashihara, M. Ueda, Sulfonated poly(ether sulfone)s with binaphthyl units as proton exchange membranes for fuel cell application, J. Polym. Sci., Part A: Polym. Chem. 47 (2009) 5827-5834.

[15] C. Klaysom, R. Marschall, L. Wang, B.P. Ladewig, G.Q.M. Lu, Synthesis of composite ion-exchange membranes and their electrochemical properties for desalination applications, J. Mater. Chem. 20 (2010) 4669-4674.

[16] Y. Shen, X. Qiu, J. Shen, J. Xi, W. Zhu, PVDF-g-PSSA and Al_2O_3 composite proton exchange membranes, J. Power Sources, 161 (2006) 54-60.

[17] P.T. Nonjola, M.K. Mathe, R.M. Modibedi, Chemical modification of polysulfone: Composite anionic exchange membrane with TiO2 nano-particles, Int. J. Hydrogen Energy, 38 (2013) 5115-5121.

[18] S.M. Hosseini, P. Koranian, A. Gholami, S.S. Madaeni, A.R. Moghadassi, P. Sakinejad, A.R. Khodabakhshi, Fabrication of mixed matrix heterogeneous ion exchange membrane by multiwalled carbon nanotubes: Electrochemical characterization and transport properties of mono and bivalent cations, Desalination, 329 (2013) 62-67.

[19] N. Hasanabadi, S.R. Ghaffarian, M.M. Hasani-Sadrabadi, Magnetic field aligned nanocomposite proton exchange membranes based on sulfonated poly (ether sulfone) and Fe_2O_3 nanoparticles for direct methanol fuel cell application, Int. J. Hydrogen Energy, 36 (2011) 15323-15332.

[20] S.M. Hosseini, M. Askari, P. Koranian, S.S. Madaeni, A.R. Moghadassi, Fabrication and electrochemical characterization of PVC based electrodialysis heterogeneous ion exchange membranes filled with Fe_3O_4 nanoparticles, J. Ind. Eng. Chem. 20 (2014) 2510-2520.

[21] A.S. Teja, P.-Y. Koh, Synthesis, properties, and applications of magnetic iron oxide nanoparticles, Prog. Cryst. Growth Charact. Mater. 55 (2009) 22-45.

[22] S. Laurent, D. Forge, M. Port, A. Roch, C. Robic, L. Vander Elst, R.N. Muller, Magnetic iron oxide nanoparticles: synthesis, stabilization, vectorization, physicochemical characterizations, and biological applications, Chem. Rev. 108 (2008) 2064-2110.

[23] R.D. Zysler, D. Fiorani, A.M. Testa, Investigation of magnetic properties of interacting Fe2O3 nanoparticles, J. Magn. Magn. Mater. 224 (2001) 5-11.

[24] B.A. Zasónska, N. Boiko, O. Klyuchivska, M. Trchová, E. Petrovský, R. Stoika, D. Horák, Silica-Coated γ-Fe2O3 Nanoparticles: Preparation and Engulfment by Mammalian Macrophages, J. Nanopharmaceutics Drug Delivery, 1 (2013) 182-192.

[25] S. Čampelj, D. Makovec, M. Drofenik, Functionalization of magnetic nanoparticles with 3-aminopropyl silane, J. Magn. Magn. Mater. 321 (2009) 1346-1350.

[26] C. Huang, B. Hu, Silica-coated magnetic nanoparticles modified with γ-mercaptopropyltrimethoxysilane for fast and selective solid phase extraction of trace amounts of Cd, Cu, Hg, and Pb in environmental and biological samples prior to their determination by inductively coupled plasma mass spectrometry, Spectrochim. Acta, Part B, 63 (2008) 437-444.

[27] A.-H. Lu, E.L. Salabas, F. Schüth, Magnetic nanoparticles: synthesis, protection, functionalization, and application, Angew. Chem. Int. Ed. 46 (2007) 1222-1244.

[28] G. Kickelbick, Concepts for the incorporation of inorganic building blocks into organic polymers on a nanoscale, Prog. Polym. Sci. 28 (2003) 83-114.

[29] Y. Oren, V. Freger, C. Linder, Highly conductive ordered heterogeneous ion-exchange membranes, J. Membr. Sci. 239 (2004) 17-26.

[30] D. Liu, M.Z. Yates, Tailoring the structure of S-PEEK/PDMS proton conductive membranes through applied electric fields, J. Membr. Sci. 322 (2008) 256-264.

[31] M. Eikerling, A.A. Kornyshev, A.M. Kuznetsov, J. Ulstrup, S. Walbran, Mechanisms of proton conductance in polymer electrolyte membranes, J. Phys. Chem. B, 105 (2001) 3646-3662.

[32] S.B. Brijmohan, M.T. Shaw, Magnetic ion-exchange nanoparticles and their application in proton exchange membranes, J. Membr. Sci. 303 (2007) 64-71.

[33] P. Daraei, S.S. Madaeni, N. Ghaemi, M.A. Khadivi, B. Astinchap, R. Moradian, Fouling resistant mixed matrix polyethersulfone membranes blended with magnetic nanoparticles: Study of magnetic field induced casting, Sep. Purif. Technol. 109 (2013) 111-121.

[34] K.S. Roelofs, T. Hirth, T. Schiestel, Sulfonated poly(ether ether ketone)-based silica nanocomposite membranes for direct ethanol fuel cells, J. Membr. Sci. 346 (2010) 215-226.

[35] M.M. Hasani-Sadrabadi, E. Dashtimoghadam, S.R. Ghaffarian, M.H. Hasani Sadrabadi, M. Heidari, H. Moaddel, Novel high-performance nanocomposite proton exchange membranes based on poly (ether sulfone), Renewable Energy, 35 (2010) 226-231.

[36] H. Zarrin, D. Higgins, Y. Jun, Z. Chen, M. Fowler, Functionalized graphene oxide nanocomposite membrane for low humidity and high temperature proton exchange membrane fuel cells, J. Phys. Chem. C, 115 (2011) 20774-20781.

[37] X. Zuo, S. Yu, X. Xu, R. Bao, J. Xu, W. Qu, Preparation of organic–inorganic hybrid cation-exchange membranes via blending method and their electrochemical characterization, J. Membr. Sci. 328 (2009) 23-30.

[38] K.T. Park, S.G. Kim, J.H. Chun, D.H. Jo, B.-H. Chun, W.I. Jang, G.B. Kang, S.H. Kim, K.B. Lee, Composite membranes based on a sulfonated poly(arylene ether sulfone) and proton-conducting hybrid silica particles for high temperature PEMFCs, Int. J. Hydrogen Energy, 36 (2011) 10891-10900.

[39] A.-L. Morel, S.I. Nikitenko, K. Gionnet, A. Wattiaux, J. Lai-Kee-Him, C. Labrugere, B. Chevalier, G. Deleris, C. Petibois, A. Brisson, M. Simonoff, Sonochemical Approach to the Synthesis of Fe_3O_4@SiO_2 core−shell nanoparticles with tunable properties, ACS Nano, 2 (2008) 847-856.

[40] P.I. Girginova, A.L. Daniel-da-Silva, C.B. Lopes, P. Figueira, M. Otero, V.S. Amaral, E. Pereira, T. Trindade, Silica coated magnetite particles for magnetic removal of Hg^{2+} from water, J. Colloid Interface Sci. 345 (2010) 234-240.

[41] W. M. Van Rhijn, D. E. De Vos, B. F. Sels, W. D. Bossaert, Sulfonic acid functionalised ordered mesoporous materials as catalysts for condensation and esterification reactions, Chem. Commun. (1998) 317-318.

[42] C.S. Gill, B.A. Price, C.W. Jones, Sulfonic acid-functionalized silica-coated magnetic nanoparticle catalysts, J. Catal. 251 (2007) 145-152.

[43] M.A. Zolfigol, A. Khazaei, M. Mokhlesi, F. Derakhshan-Panah, Synthesis, characterization and catalytic properties of monodispersed nano-sphere silica sulfuric acid, J. Mol. Catal. A: Chem. 370 (2013) 111-116.

[44] N.P. Gnusin, N.P. Berezina, N.A. Kononenko, O.A. Dyomina, Transport structural parameters to characterize ion exchange membranes, J. Membr. Sci. 243 (2004) 301-310.

[45] F.A. Siddiqi, I.R. Khan, S.K. Saksena, M.A. Ahsan, Studies with model membranes, J. Membr. Sci. 2 (1977) 245-261.

[46] N.P. Berezina, N.A. Kononenko, O.A. Dyomina, N.P. Gnusin, Characterization of ion-exchange membrane materials: properties vs structure, Adv. Colloid Interface Sci. 139 (2008) 3-28.